Acta Crystallographica Section F
Structural Biology and Crystallization Communications
ISSN 1744-3091

Purification, crystallization and preliminary data analysis of the ligand–receptor complex of the growth and differentiation factor 5 variant R57A (GDF5R57A) and BMP receptor IA (BRIA)

Joachim Nickel,[a] Alexander Kotzsch,[b] Walter Sebald[a] and Thomas D. Mueller[b]*

[a]Lehrstuhl für Physiologische Chemie II, Theodor-Boveri-Institut für Biowissenschaften (Biozentrum) der Universität Würzburg, Am Hubland, D-97074 Würzburg, Germany, and [b]Lehrstuhl für Botanik I – Molekulare Pflanzenphysiologie und Biophysik, Julius-von-Sachs-Institut für Biowissenschaften (Biozentrum) der Universität Würzburg, Julius-von-Sachs Platz 2, D-97082 Würzburg, Germany

Correspondence e-mail: mueller@biozentrum.uni-wuerzburg.de

Received 27 January 2011
Accepted 23 February 2011

The binary ligand–receptor complex of human growth and differentiation factor 5 (GDF5) bound to its type I receptor BMP receptor IA (BRIA) was prepared and crystallized. By utilizing the GDF5 variant R57A, which exhibits a high affinity in the subnanomolar range for BRIA, the binary complex of GDF5R57A bound to the extracellular domain of BRIA could be produced and purified. Crystals of this complex belonged to a monoclinic space group: either $I2$, with unit-cell parameters $a = 63.81$, $b = 62.85$, $c = 124.99$ Å, $\beta = 95.9^\circ$, or $C2$, with unit-cell parameters $a = 132.17$, $b = 62.78$, $c = 63.53$ Å, $\beta = 112.8^\circ$.

1. Introduction

Growth and differentiation factor 5 (GDF5) belongs to the family of transforming growth factors (TGF-β) and drives important processes in the developing skeleton, in particular the formation of joints (Buxton *et al.*, 2001; Edwards & Francis-West, 2001; Luyten, 1997). Genetic studies have identified a number of genes as being crucial for joint formation, such as the growth factors *wnt9a* and *wnt4*, the BMP modulator *noggin* and *gdf5* (Brunet *et al.*, 1998; Hartmann & Tabin, 2001; Storm *et al.*, 1994). Mutations in the *gdf5* gene result in defects in wrist, ankle and digit joints, attesting to the chondrogenic activity of GDF5. Noggin is a factor displaying antichondrogenic activity that can directly antagonize GDF5 activity by binding to GDF5. GDF5 binds and oligomerizes two types of single transmembrane serine/threonine receptor kinases referred to as type I and type II receptors (Massagué, 1998; Heldin *et al.*, 1997). Upon the formation of a heteromeric receptor complex comprising the dimeric GDF5 and two type I as well as two type II receptors, an intracellular phosphorylation cascade activates members of the SMAD family of transcription factors, which then directly act on target genes in the cell.

Whereas many ligands of the TGFβ family exhibit highly promiscuous binding to various receptors of the type I and type II subfamilies (Sebald *et al.*, 2004; Nickel *et al.*, 2009; Heinecke *et al.*, 2009), proper biological function of GDF5 *in vivo* seems to depend strictly on the type I receptor BRIB. *In vitro* studies have shown that GDF5 is nonetheless capable of binding to both type I receptors BRIA and BRIB with a difference in binding affinity (K_d for GDF5–BRIB, 1 nM; K_d for GDF5–BRIA, 19–20 nM) of about 20-fold (Nickel *et al.*, 2005; Heinecke *et al.*, 2009; Kotzsch *et al.*, 2009). Mutations in GDF5 that alter this type I receptor specificity, such as R57L, have been found in patients suffering from DuPan syndrome, a form of symphalangism characterized by the fusion of interphalangal joints in fingers IV and V (Seemann *et al.*, 2005). Importantly, the distinct expression patterns of the BMP type I receptors BRIA and BRIB highlight their role in joint development. In the limbs, BRIA expression is highly restricted to joint interzones, whereas BRIB is expressed in the regions flanking the joint interzones (Baur *et al.*, 2000). Concordantly, BRIB knockout mice show defects in joint formation reminiscent of those seen in *gdf5*$^{-/-}$ mice (Yi *et al.*, 2000; Storm & Kingsley, 1996).

Our efforts to analyse the structures of GDF5–type I receptor complexes were motivated by two main questions. Firstly, how can GDF5 generate type I receptor specificity towards BRIB? Secondly, are there differences in the ligand–receptor assembly that possibly

account for the differences in signalling? Here, we present the preparation and preliminary crystal analysis of the binary complex of the GDF5 variant R57A bound to the extracellular domain of the type I receptor BRIA.

2. Materials and methods

2.1. Protein expression and purification

The extracellular domain of human BRIA ($BRIA_{EC}$; residues 1–129; Swiss-Prot 36894) was expressed as a thioredoxin fusion in the cytoplasm of *Escherichia coli* strain AD494 (DE3) as described in Kirsch *et al.* (2000). Transformed *E. coli* cells were grown at 310 K to an optical density of 0.4 at 550 nm and then cooled to 293 K. After keeping the cell culture at 293 K for 30 min, protein expression was induced by adding IPTG (final concentration of 1 m*M*). Protein expression was continued overnight at 293 K. After protein expression, cells were harvested by centrifugation and the pellet was resuspended in 20 m*M* Tris pH 7.9, 500 m*M* NaCl, 20 m*M* imidazole. The bacterial cells were lysed by sonication and the clarified supernatant was subjected to metal-ion affinity chromatography using Ni^{2+}–NTA resin. Crude $BRIA_{EC}$ protein was eluted using 500 m*M* imidazole and dialyzed first against 50 m*M* Tris pH 7.5, 150 m*M* NaCl and 1 m*M* EDTA to remove residual nickel ions and then against 50 m*M* Tris pH 7.5, 150 m*M* NaCl and 2.5 m*M* $CaCl_2$ for thrombin cleavage of the fusion protein. The Trx-$BRIA_{EC}$ fusion protein was cleaved using 0.3 U thrombin (Sigma) per milligram of Trx-$BRIA_{EC}$ until proteolysis was complete (5–6 h at 303 K). To increase the yield of monomeric active $BRIA_{EC}$, the reaction mixture was incubated after enzymatic proteolysis for 72–96 h at 277 K. Thioredoxin, monomeric and multimeric $BRIA_{EC}$ were separated by anion-exchange chromatography using EMD-TMAE (Merck) as the column resin. The proteolysis mixture was dialyzed against 20 m*M* Tris pH 7.5, 35 m*M* NaCl and subsequently applied onto the column. The proteins were then separated by a linear gradient from 35 m*M* to 1 *M* NaCl in 50 m*M* Tris pH 7.5. Highly pure $BRIA_{EC}$ protein was obtained employing affinity chromatography using a BMP-2 affinity matrix (BMP-2 coupled to CNBr-activated Sepharose; GE Healthcare).

The variant GDF5R57A (residues 381–501; Swiss-Prot 43206) was obtained by PCR mutagenesis using the QuikChange methodology (Weiner & Costa, 1994). The expression plasmid $RBSII_{N25}$x/o encoding the mature part of human GDF5R57A was then transformed into *E. coli* strain BL21 (DE3). Transformed bacteria were grown at 310 K to an optical density of 0.6 at 550 nm, at which point protein expression was induced by addition of IPTG (final concentration of 1 m*M*). Expression was continued for 3 h at 310 K. The cells were harvested by centrifugation and lysed by sonication. GDF5R57A was isolated from inclusion bodies and dissolved in 6 *M* guanidine hydrochloride at a protein concentration of 10–20 mg ml^{-1}. For refolding, the protein solution was then diluted 1:100 in 2 *M* LiCl, 50 m*M* Tris pH 8.0, 33 m*M* CHAPS and 2 m*M* of the redox couple glutathione in reduced and oxidized form (ratio 4:1). Completion of GDF5R57A folding was judged from quantification of the GDF5 dimer formation as seen by SDS–PAGE. To isolate the GDF5R57A dimer, the refolding mixture was first dialyzed against 1 m*M* HCl. The protein solution was then mixed with 2-propanol and 1 *M* sodium acetate pH 4.5 to a final concentration of 30% 2-propanol and 20 m*M* sodium acetate pH 4.5 prior to cation-exchange chromatography using SP-Sepharose as resin. Dimeric pure GDF5R57A was eluted from the column using a linear gradient of 0–2 *M* NaCl in 20 m*M* sodium acetate pH 4.5 and 30% 2-propanol. Fractions containing pure dimeric GDF5R57A were dialyzed against water and stored at 253 K until further use.

2.2. Preparation and crystallization of the ligand–receptor complexes

The complex of GDF5R57A bound to $BRIA_{EC}$ was prepared by mixing GDF5R57A with two molar equivalents of $BRIA_{EC}$. 44 nmol $BRIA_{EC}$ dissolved in 400–500 µl water was initially mixed with 4× HBS buffer (40 m*M* HEPES pH 7.4, 2 *M* NaCl) to yield a receptor-protein solution in 2× HBS buffer (20 m*M* HEPES pH 7.4, 1 *M* NaCl). 20 nmol GDF5R57A was dissolved in water or 1 m*M* HCl to a concentration of 5 µ*M*. The binary complex was then formed by adding the GDF5R57A solution rapidly to the BRIA solution under vigorous vortexing followed by incubation of the protein solution for 20 min at 294 K. Precipitate was removed by centrifugation and the complex was concentrated by ultrafiltration to a final volume of 250 µl. Removal of excess receptor protein was accomplished by gel filtration using HBS_{500} buffer (10 m*M* HEPES pH 7.4, 500 m*M* NaCl) employing a Superdex 75 HR10/30 column (GE Healthcare). Fractions were analyzed with respect to the stoichiometry of the complex components by SDS–PAGE using standards for the ligand and

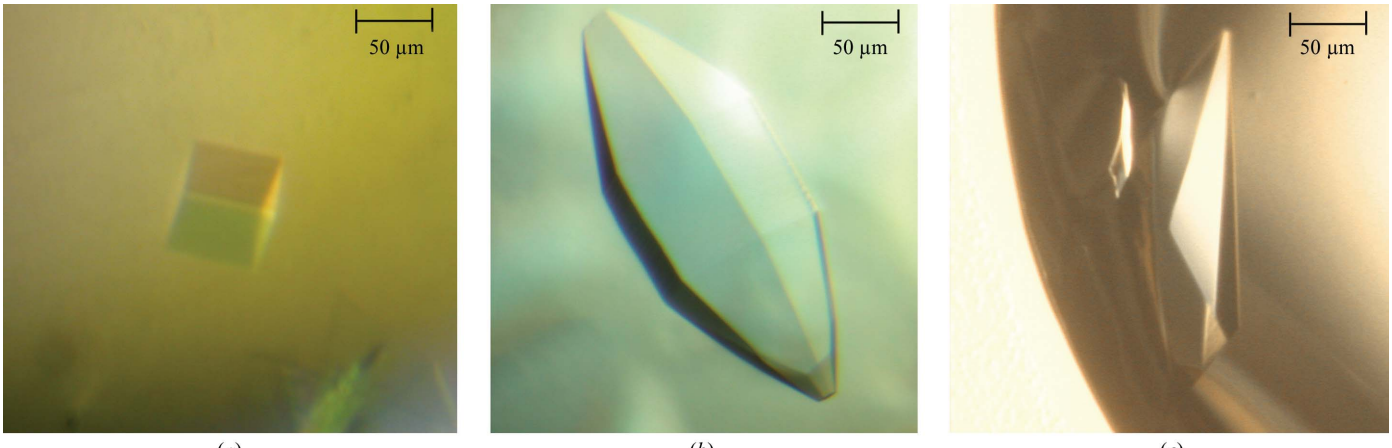

(*a*) (*b*) (*c*)

Figure 1
Different morphologies of crystals of the GDF5R57A–$BRIA_{EC}$ complex. (*a*) Cubic-shaped crystals grew to dimensions of 80 × 80 × 80 µm within two weeks. (*b*) Hexahedral bipyramidal crystals grew to larger dimensions of about 500 × 150 × 100 µm. (*c*) Only crystals exhibiting a skewed hexahedral/rhombohedral crystal form (dimensions of about 300 × 200 × 80 µm) diffracted X-rays to high resolution.

receptor protein. Fractions containing the GDF5R57A–$BRIA_{EC}$ complex with a 1:2 stoichiometry were pooled and concentrated to 18 mg ml^{-1} *via* ultrafiltration in HBS_{500} buffer (10 m*M* HEPES pH 7.5, 500 m*M* NaCl).

Initial crystallization trials were set up manually using Greiner 96-well CrystalQuick plates employing sitting-drop vapour diffusion. 1 µl protein solution was mixed with 1 µl reservoir solution; to optimize the concentration of the protein complex for crystallization, four different concentrations (18, 15, 10 and 8 mg ml^{-1}) were tested. All crystallization trials were performed at 294 K using a temperature-controlled incubator. Initial sparse-matrix screening (using Hampton Research SaltRx, PEG/Ion and Index screens) yielded several conditions providing needle clusters or single crystals, mostly involving salts, *e.g.* magnesium formate or ammonium citrate, or polyethylene glycols, *e.g.* polyethylene glycol monomethyl ether 5000 or PEG 3350, as precipitants and employing pH values between 5.5 and 8.0. The most successful screening was obtained using Index screen, where needle clusters or even large single crystals could be grown in 11 out of 96 conditions (Index screen condition Nos. 15, 22, 43, 46, 70, 71, 72, 83, 90 and 95). Optimization of the initial crystallization conditions was performed for the conditions (Index screen condition Nos. 43, 70, 71, 72, 83 and 90) that employed PEG 3350 as precipitant with either Bis-Tris or HEPES as a buffer component. Besides buffer chemistry, a pH range between 6.0 and 8.0 was tested. Furthermore, as the initial conditions contained different salts, *e.g.* sodium chloride, magnesium chloride and sodium formate, the effect of each of these additives on crystallization was tested using different concentrations (varied between 0.05 and 0.2 *M*). Optimization screening was performed using a hanging-drop vapour-diffusion setup and MDL XRL 24-well plates. The ratio of protein solution to reservoir solution in the droplet was 1:1, with 2 µl droplets for screening and 4 µl droplets for the production of crystals for data acquisition. Crystallization using PEGs as precipitant yielded three predominant crystal forms: smaller cube-shaped crystals, large crystals with a hexagonal bipyramidal form and skewed hexahedral form crystals (Fig. 1). Only crystals of the latter form diffracted X-rays to high resolution. Crystals with hexahedral morphology reaching dimensions of up to 300 × 200 × 80 µm were obtained within four weeks at 294 K from 0.1 *M* Bis-Tris or HEPES pH 6.5–8.0, 0.2 *M* NaCl and 18–25%(*w*/*v*) PEG 3350. These crystals diffracted to 2.2 Å resolution (Fig. 2). For data acquisition, crystals were grown from 0.1 *M* HEPES pH 7.5, 0.2 *M* NaCl, 20%(*w*/*v*) PEG 3350 and were soaked for 30 s in crystallization solution containing 30%(*w*/*v*) PEG 3350 before freezing in liquid nitrogen to avoid icing.

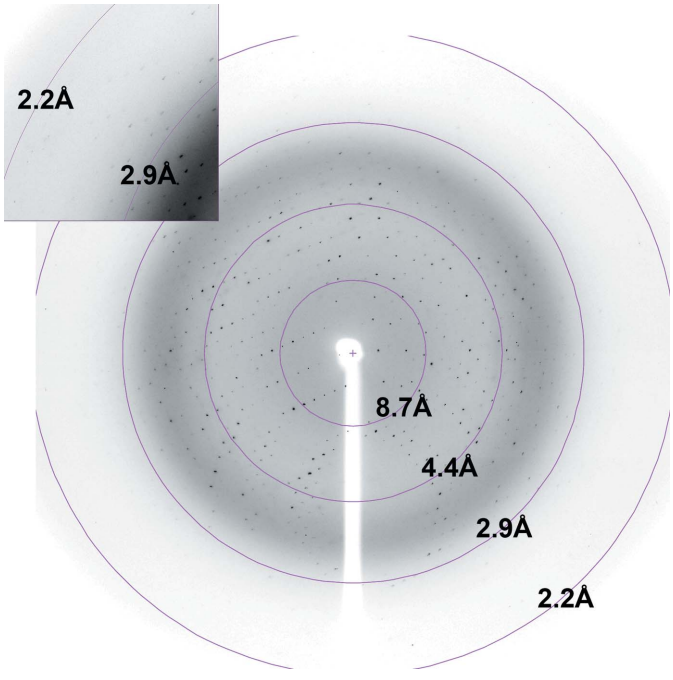

Figure 2
Diffraction pattern of the crystal in Fig. 1(*c*) comprising the binary complex of GDF5R57A bound to the extracellular domain of the BMP type I receptor BRIA. The diffraction limit of these crystals was about 2.3 Å.

Table 1
Data-collection and processing statistics for the native crystals of GDF5R57A–$BRIA_{EC}$.

Values in parentheses are for the highest resolution shell.

	Home-source data set	Synchrotron data set
Detector	R-AXIS IV^{++}	MAR 225 Mosaic
Space group	*I*2	*I*2
Temperature (K)	100	100
Unit-cell parameters (Å, °)	a = 63.81, b = 62.85, c = 124.99, $\alpha = \gamma$ = 90, β = 95.85	a = 63.90, b = 62.89, c = 125.43, $\alpha = \gamma$ = 90, β = 95.85
Wavelength (Å)	1.15418	1.1048
Resolution (Å)	24.0–2.28 (2.40–2.28)	17.20–2.36 (2.49–2.36)
No. of reflections (total/unique)	51824/22044	46989/19986
Completeness (%)	97.8 (97.4)	97.7 (97.5)
Multiplicity	2.4 (2.4)	2.4 (2.4)
R_{merge}† (%)	6.6 (38.4)	6.1 (28.5)
$\langle I/\sigma(I)\rangle$	7.4 (2.0)	7.5 (2.4)
No. of complexes per asymmetric unit	1	1
Matthews coefficient (Å^3 Da^{-1})	2.3	2.3
Solvent content (%)	46.8	46.8

† $R_{merge} = \sum_{hkl}\sum_i |I_i(hkl) - \langle I(hkl)\rangle| / \sum_{hkl}\sum_i I_i(hkl)$, where $I_i(hkl)$ is the intensity of the ith observation of the unique reflection hkl and $\langle I(hkl)\rangle$ is the the mean of the intensities of all observations of reflection hkl.

2.3. Data collection

Two native data sets were collected, one using a home source and a second using beamline XS06 at the Swiss Light Source (Villigen, Switzerland). Smaller crystals (up to 100 × 80 × 30 µm) were directly flash-frozen in liquid nitrogen, while larger crystals were soaked in crystallization reservoir solution containing 30%(*w*/*v*) PEG 3350. Data acquisition using the home source (Rigaku MicroMax-007, VariMax Cu HighRes mirror optics and a Rigaku R-AXIS IV^{++} image-plate system) was performed using a crystal-to-detector distance of 130 mm; the wavelength was 1.5418 Å and data collection was performed at 100 K, rotating the crystal through 123° (0.5° oscillation) with 360 s exposure per frame. A second data set was acquired on beamline XS06 (SLS Villigen, Switzerland) with the crystal-to-detector distance set to 200 mm; the wavelength was 1.1048 Å and crystals were rotated through a total of 150° with 1° oscillation and an exposure of 1 s per frame. Data processing was performed using *CrystalClear* (Rigaku–MSC), *iMOSFLM*/*MOSFLM* (Leslie, 1992) and *SCALA* from the *CCP*4 package (Collaborative Computational Project, Number 4, 1994).

3. Results and discussion

Crystals of the ligand–receptor complex of the GDF5 variant R57A bound to the ectodomain $BRIA_{EC}$ could be obtained from several crystallization conditions containing salts (magnesium formate or ammonium citrate) or polyethylene glycol (molecular-weight range 2000–5000) at pH values ranging from slightly acidic to slightly basic.

Table 2
Molecular replacement using *Phaser* and initial refinement.

Multi-template search using *Phaser* and dimeric GDF5 (PDB entry 1waq) as ensemble 1 and $BRIA_{EC}$ (PDB entry 1rew chain *C*) as ensemble 2. The run was set up to search for one dimeric GDF5 and two $BRIA_{EC}$ molecules in the asymmetric unit of the GDF5R57A–$BRIA_{EC}$ crystal. RFZ is the *Z* score of the rotation function, TFZ is the *Z* score of the translation function and LLG is the log-likelihood gain; *Z*-score values of greater than 8 in the rotation and translation function indicate correct solutions for the molecular-replacement run. For correct solutions of the molecular-replacement run the values for log-likelihood gain should be large and positive and in the multi-ensemble setup the value should increase upon adding another template to the search run.

Template	Data processed in space group *C*2	Data processed in space group *I*2
GDF5 dimer	RFZ = 15.6, TFZ = 15.8, LLG = 396	RFZ = 15.3, TFZ = 12.3, LLG = 397
BRIA molecule 1	RFZ = 9.8, TFZ = 21.1, LLG = 974	RFZ = 9.5, TFZ = 29.3, LLG = 963
BRIA molecule 2	RFZ = 7.2, TFZ = 25.0, LLG = 1408	RFZ = 7.0, TFZ = 25.1, LLG = 1396
Rigid-body refinement†	R_{cryst} = 44%, R_{free} = 44%, FOM‡ = 0.46	R_{cryst} = 44%, R_{free} = 44%, FOM = 0.55
First refinement round§	R_{cryst} = 31.2%, R_{free} = 35.5%, FOM = 0.67	R_{cryst} = 30.4%, R_{free} = 34.7%, FOM = 0.73
Second refinement round§	R_{cryst} = 28.3%, R_{free} = 32.7%, FOM = 0.70	R_{cryst} = 27.0%, R_{free} = 32.2%, FOM = 0.75

† Rigid-body refinement defining each chain of the GDF5 dimer and the two $BRIA_{EC}$ molecules as independent rigid bodies. ‡ Figure of merit. § First and second round of manual model building and subsequent 20 cycles of restrained refinement using *REFMAC* v.5.02.

To obtain a stable and highly concentrated protein solution, the binary complex GDF5R57A–$BRIA_{EC}$ was formed in HBS_{500} buffer and concentrated in this high ionic strength buffer *via* ultrafiltration subsequent to purification by gel filtration. To check for the presence of the protein complex, crystals were harvested, washed in order to remove adhering protein solution and their composition was analyzed by SDS–PAGE. With the exception of rather acidic conditions (pH $\leq$ 4), all of these crystallization conditions produced crystals containing ligand and receptor protein in the expected 1:2 molar stoichiometry. Large single crystals could be grown from 18–25%(*w*/*v*) PEG 3350, 0.2 *M* sodium chloride and a neutral to slightly basic pH ranging from pH 6.5 to 8.5 using either Bis-Tris, HEPES or Tris as buffers. Interestingly, crystals of three distinct morphologies (a cubic hexahedral form, large crystals exhibiting a regular hexagonal bipyramidal form and crystals of a skewed hexahedral/rhombohedral form) were obtained despite the small differences in the crystallization conditions. Only crystals of the latter morphology diffracted X-rays to high resolution (up to 2.2 Å). For data acquisition, crystals of GDF5R57A–$BRIA_{EC}$ were grown at 294 K from 18%(*w*/*v*) PEG 3350, 0.2 *M* sodium chloride, 0.1 *M* HEPES pH 8.0; the protein concentration for the complex was 18 mg ml^{-1}. For cryoprotection, the protein crystals were soaked for 30 s in reservoir solution containing 30%(*w*/*v*) PEG 3350 just before cryocooling.

Two complete native data sets could be acquired. The first data set was collected from a single crystal at 100 K using a home source. The data from 123 0.5° frames consisted of 22 742 unique reflections. The overall R_{merge} was 6.4% for the resolution range 31.6–2.28 Å and the completeness was 98.6%. Indexing and scaling of the data using *CrystalClear* v.1.3.6 (Rigaku–MSC) suggested that the crystal belonged to the monoclinic space group *C*2, with unit-cell parameters a = 135.03, b = 63.81, c = 64.20 Å, β = 111.95° (Table 1). Calculation of the Matthew coefficient (Matthews, 1968; V_M = 2.35 $Å^3$ Da^{-1}, solvent content 47.8%) and the appearance of non-origin/noncrystallographic symmetry peaks in Patterson maps from self-rotation analysis using *MOLREP* (Vagin & Teplyakov, 2010) at the κ = 180° section suggested the presence of the full complex comprising the homodimeric ligand GDF5R57A bound to two $BRIA_{EC}$ moieties in the asymmetric unit of the crystal. To solve the structure of the complex, we employed molecular replacement using *Phaser* (McCoy *et al.*, 2007) and the structures of wild-type dimeric GDF5 (PDB entry 1waq; Nickel *et al.*, 2005) and of the extracellular domain of BRIA (chain *C* of PDB entry 1rew; Keller *et al.*, 2004) as search templates. The rotation and translation searches were performed in a stepwise procedure, first calculating the orientation and location of the ligand dimer and subsequently that of the $BRIA_{EC}$ molecule(s). A clear molecular-replacement solution allowed placement of the dimeric GDF5 ligand bound to two $BRIA_{EC}$ moieties in the asymmetric unit (Table 2). However, iterative refinement runs comprising manual rebuilding using *QUANTA*2006 (Accelrys MSI) and subsequent refinement using *REFMAC*5 (Murshudov *et al.*, 1997) did not lead to R_{free} values below 30%.

Data analysis ruled out twinning as a possible issue for the remaining high R_{free} value. We thus acquired a second data set from another crystal on the XS06 synchrotron beamline (SLS Villigen, Switzerland). This data set was obtained from a single crystal at 100 K and consisted of 150 1° frames. Processing with *CrystalClear* v.1.3.6 (Rigaku–MSC) suggested that the crystal belonged to space group *C*2, with similar unit-cell parameters as observed for the data set acquired at the home source. However, processing using *MOSFLM* (Leslie, 1992) together with *POINTLESS* (Evans, 2006) and *SCALA* (Collaborative Computational Project, Number 4, 1994) suggested a different indexing of the diffraction data, indicating that the crystal belonged to space group *I*2, with unit-cell parameters a = 63.90, b = 62.89, c = 125.43 Å, β = 95.85°. Similarly, reprocessing the data set acquired at the home source using *MOSFLM*, *POINTLESS* and *SCALA* showed that the same indexing can also be applied to this data set, yielding space group *I*2 with unit-cell parameters a = 63.81, b = 62.85, c = 124.99 Å, β = 95.85° (see also Table 1). Repeating molecular replacement and refinement with the reprocessed data set as described above now led to R_{free} values of less than 30% after several rounds of refinement. At present we are completing the refinement of the structure, which will provide important insights into how GDF5 discriminates between the BMP type I receptors BRIA and BRIB.

The authors gratefully acknowledge access to synchrotron beamline X06SA at SLS (Villigen) and to the X-ray facility at the Rudolf-Virchow Center at Würzburg University. The authors would also like to thank Maike Gottermeier for excellent technical assistance, Werner Schmitz for mass-spectrometric analyses and Stefan Saremba for critical reading of the manuscript. This research is supported by the Deutsche Forschungsgemeinschaft SFB 487 B2.

References

Baur, S. T., Mai, J. J. & Dymecki, S. M. (2000). *Development*, **127**, 605–619.
Brunet, L. J., McMahon, J. A., McMahon, A. P. & Harland, R. M. (1998). *Science*, **280**, 1455–1457.
Buxton, P., Edwards, C., Archer, C. W. & Francis-West, P. (2001). *J. Bone Joint Surg. Am.* **83**, S23–S30.
Collaborative Computational Project, Number 4 (1994). *Acta Cryst.* D**50**, 760–763.
Edwards, C. J. & Francis-West, P. H. (2001). *Semin. Arthritis Rheum.* **31**, 33–42.

Evans, P. (2006). *Acta Cryst.* D**62**, 72–82.
Hartmann, C. & Tabin, C. J. (2001). *Cell*, **104**, 341–351.
Heinecke, K., Seher, A., Schmitz, W., Mueller, T. D., Sebald, W. & Nickel, J. (2009). *BMC Biol.* **7**, 59.
Heldin, C. H., Miyazono, K. & ten Dijke, P. (1997). *Nature (London)*, **390**, 465–471.
Keller, S., Nickel, J., Zhang, J.-L., Sebald, W. & Mueller, T. D. (2004). *Nature Struct. Mol. Biol.* **11**, 481–488.
Kirsch, T., Nickel, J. & Sebald, W. (2000). *FEBS Lett.* **468**, 215–219.
Kotzsch, A., Nickel, J., Seher, A., Sebald, W. & Müller, T. D. (2009). *EMBO J.* **28**, 937–947.
Leslie, A. G. W. (1992). *Jnt CCP4/ESF–EACBM Newsl. Protein Crystallogr.* **26**.
Luyten, F. P. (1997). *Oral Surg. Oral Med. Oral Pathol. Oral Radiol. Endod.* **83**, 167–169.
Massagué, J. (1998). *Annu. Rev. Biochem.* **67**, 753–791.
Matthews, B. W. (1968). *J. Mol. Biol.* **33**, 491–497.
McCoy, A. J., Grosse-Kunstleve, R. W., Adams, P. D., Winn, M. D., Storoni, L. C. & Read, R. J. (2007). *J. Appl. Cryst.* **40**, 658–674.
Murshudov, G. N., Vagin, A. A. & Dodson, E. J. (1997). *Acta Cryst.* D**53**, 240–255.
Nickel, J., Kotzsch, A., Sebald, W. & Mueller, T. D. (2005). *J. Mol. Biol.* **349**, 933–947.
Nickel, J., Sebald, W., Groppe, J. C. & Mueller, T. D. (2009). *Cytokine Growth Factor Rev.* **20**, 367–377.
Sebald, W., Nickel, J., Zhang, J.-L. & Mueller, T. D. (2004). *Biol. Chem.* **385**, 697–710.
Seemann, P., Schwappacher, R., Kjaer, K. W., Krakow, D., Lehmann, K., Dawson, K., Stricker, S., Pohl, J., Plöger, F., Staub, E., Nickel, J., Sebald, W., Knaus, P. & Mundlos, S. (2005). *J. Clin. Invest.* **115**, 2373–2381.
Storm, E. E., Huynh, T. V., Copeland, N. G., Jenkins, N. A., Kingsley, D. M. & Lee, S. J. (1994). *Nature (London)*, **368**, 639–643.
Storm, E. E. & Kingsley, D. M. (1996). *Development*, **122**, 3969–3979.
Vagin, A. & Teplyakov, A. (2010). *Acta Cryst.* D**66**, 22–25.
Weiner, M. P. & Costa, G. L. (1994). *PCR Methods Appl.* **4**, S131–S136.
Yi, S. E., Daluiski, A., Pederson, R., Rosen, V. & Lyons, K. M. (2000). *Development*, **127**, 621–630.